Chemical Science

EDGE ARTICLE

View Article Online
View Journal | View Issue

Cite this: *Chem. Sci.*, 2017, **8**, 5005

Discrimination of supramolecular chirality using a protein nanopore†

James A. Cooper, Stefan Borsley, Paul J. Lusby and Scott L. Cockroft *

Supramolecular chirality may emerge from self-assembly processes to yield architectures that differ only in the topological arrangement of their constituent parts. Since the properties of the resulting enantiomeric assemblies are identical, purification and characterisation can be challenging. Here, we have examined the hypothesis that the intrinsic chirality of a protein nanopore can be exploited to detect supramolecular chirality. Transient blockages in the ion current flowing through a single membrane-spanning α-haemolysin nanopore were shown to discriminate between M_4L_6 tetrahedral coordination cages of opposing chiralities. The single-molecule nature of the approach facilitated direct access to the rates of association and dissociation with the nanopore, which allowed the concentrations of the enantiomeric supramolecular assemblies to be determined *in situ*. Thus, we have established that a protein nanopore can be used to discriminate the chiral topologies of supramolecular assemblies, even when they are too large to fully enter the nanopore.

Received 1st May 2017
Accepted 4th May 2017

DOI: 10.1039/c7sc01940h

rsc.li/chemical-science

Introduction

Chirality is ubiquitous in chemistry and biology. As such, the discrimination and separation of stereoisomers is vital. Diastereotopic relationships have long been exploited to discriminate between stereoisomers. For example, covalent derivatisation with chiral reagents can be used to distinguish between chiral centres that are identical in every other regard. Diastereotopic relationships can also be manifested in a non-covalent supramolecular context, as illustrated by stereoselective synthesis,[1] chiral HPLC[2] and the use of chiral shift agents in NMR spectroscopy.[3,4] However, the control and characterisation of supramolecular chirality in self-assembled systems[5,6] becomes more challenging as chemists seek to construct increasingly complicated assemblies.[7,8] Indeed, the expression, recognition and control of supramolecular chirality is essential for life.[9–12] Bringing together these biological and synthetic supramolecular aspects,[13] we reasoned that intrinsically chiral transmembrane protein nanopores might be utilised as detectors of supramolecular chirality.

Here we have examined the utility of an α-haemolysin (α-HL) protein nanopore to discriminate the supramolecular chirality of tetrahedral coordination cages (Fig. 1). Enantiopure cages, and mixtures thereof, were interrogated at the single-molecule level by monitoring changes in the transmembrane ion current passing through a single protein pore under an applied potential (Fig. 2). Differences between the magnitudes of the ion current blockages (Fig. 2 and 5), and the kinetics and thermodynamics of binding (Fig. 3) were evaluated for both chiral forms of the supramolecular cage and discussed in the context of the relative dimensions of the cage complex and the nanopore (Fig. 4).

Chirality is a key aspect in biological signal transduction[14,15] that has inspired synthetic transmembrane messengers.[16,17] Similarly, the chiral discrimination of molecules small enough

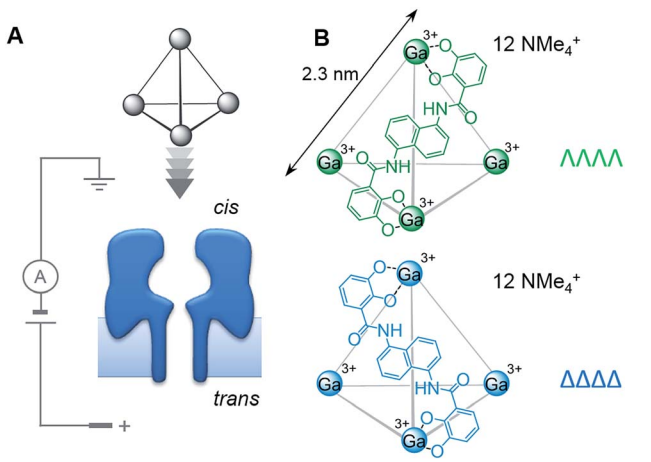

Fig. 1 (A) Experimental setup in which tetrahedral coordination cages were driven towards the *cis*-opening of a single α-haemolysin (α-HL) nanopore inserted in a lipid bilayer under an applied transmembrane potential. (B) ΛΛΛΛ (green) and ΔΔΔΔ (blue) homochiral forms of the Ga(III) cage used in this study. Each grey edge indicates the position of a bridging ligand molecule.

EaStCHEM School of Chemistry, University of Edinburgh, Joseph Black Building, David Brewster Road, Edinburgh EH9 3FJ, UK. E-mail: scott.cockroft@ed.ac.uk

† Electronic supplementary information (ESI) available: Synthesis, characterisation, methods and supplementary data. See DOI: 10.1039/c7sc01940h

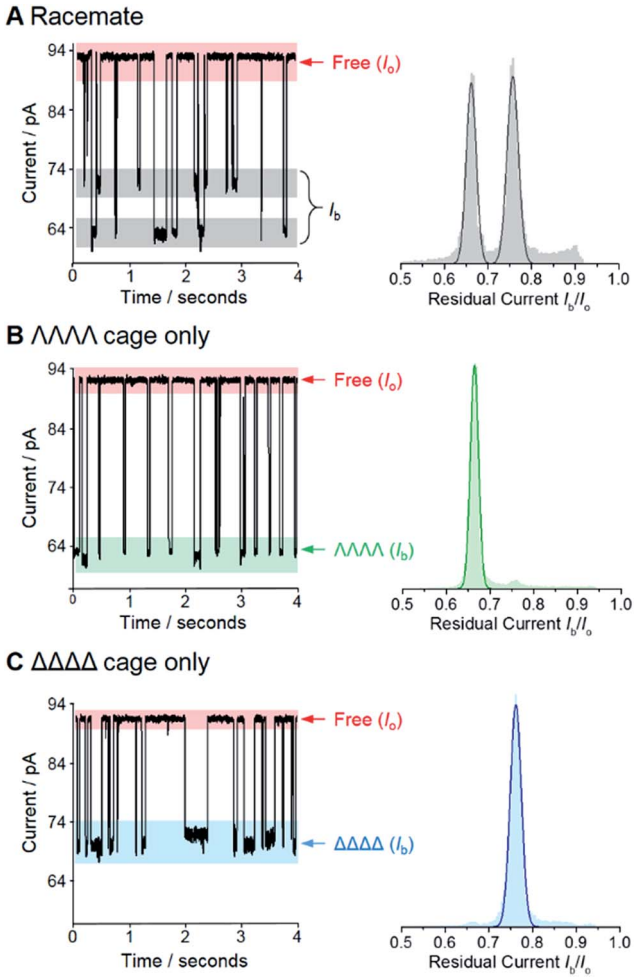

Fig. 2 Enantiodiscrimination of Ga(III) coordination cages by an α-HL nanopore at +100 mV. Representative ion current traces and corresponding event histograms for nanopore analysis of (A) a racemic mixture of the coordination cage, (B) enantiopure ΛΛΛΛ cage, and (C) enantiopure ΔΔΔΔ cage. Each histogram was generated from at least six different experiments totaling >34 000 events in each case. Experiments were performed in 1 M KCl, 30 mM Tris–DCl, pD 7.6 in D_2O at 293 ± 2 K with an applied potential of +100 mV.

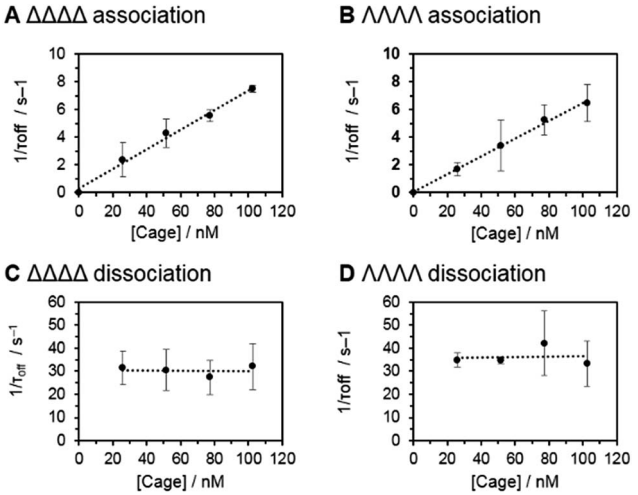

Fig. 3 (A–D) Association and dissociation kinetics of the ΔΔΔΔ and ΛΛΛΛ cages with an α-HL nanopore. The rate constant k_{on} was obtained from the slope of the linear fit of $1/\tau_{on}$ *versus* [cage] for ΔΔΔΔ (A) and ΛΛΛΛ (B). The rate constant k_{off} was obtained from the intercept of the graph $1/\tau_{off}$ *versus* [cage] for ΔΔΔΔ (C) and ΛΛΛΛ (D). Experiments were performed in 1 M KCl, 30 mM Tris–DCl, pD 7.6 in D_2O at 293 ± 2 K with an applied potential of +100 mV.

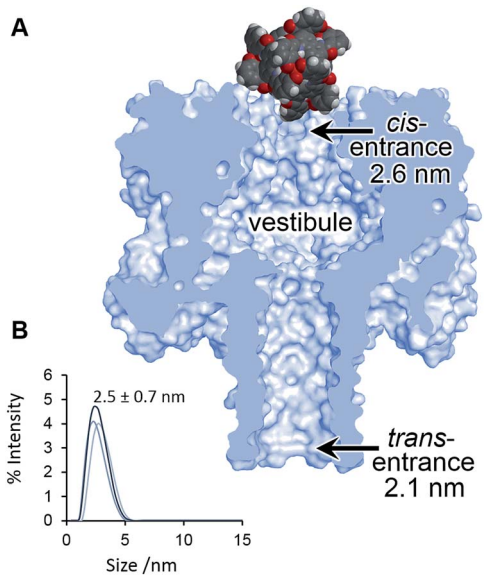

Fig. 4 (A) Scaled model of a Ga(III) cage complex overlaid with the crystal structure of α-HL.[44] (B) Dynamic light scattering measurement of a racemic sample of the Ga(III) cage complex in D_2O 293 ± 2 K.

to enter membrane-spanning nanopores has been previously demonstrated.[18–27] To date, it is not yet known whether nanopore-based chiral sensors are amenable to the study of larger supramolecular assemblies, particularly those that are too large to enter the nanopore. Furthermore, the advantage of using atomically precise protein nanopores in the enantiodetection of small molecules has been counterbalanced by the need to employ genetically modified proteins.[18–20]

Results and discussion

We selected the pairing of the transmembrane protein nanopore, wild-type α-haemolysin (α-HL), and a previously reported chiral Ga(III) cage for our investigation of supramolecular enantiodiscrimination (Fig. 1).[28] These coordination cages possess supramolecular chirality due to the two possible propeller-like arrangements of the ligands around each metal centre (ΛΛΛΛ and ΔΔΔΔ, Fig. 1B). Like many other cages constructed from rigid bis(bidentate) ligands and octahedral metal ions, these complexes assemble exclusively as the homochiral racemate at the expense of the other possible diastereoisomers.[29–36] It has previously been established that the selected Ga(III) tetrahedral cages are water soluble, and that conversion between the homochiral forms is negligible under basic conditions.[37] The cages bear twelve negative charges meaning that they can be driven towards the nanopore under an applied electric field.[38] Furthermore, the dimensions of the

tetrahedral cage and the *cis*-opening of α-HL nanopore are similar (~2.3 nm *vs.* ~2.6 nm).

At the start of our investigations we synthesised a racemic mixture of the tetrahedral cages[28] for nanopore analysis. In the initial nanopore experiments, a planar lipid bilayer was painted across a 100 μm aperture separating two wells of buffered solution (1 M KCl, 30 mM Tris–DCl, pD 7.6 in D_2O‡). A single α-HL nanopore was introduced into the bilayer,[39] as indicated by the characteristic ionic current flowing through the nanopore at an applied transmembrane voltage of +100 mV (I_o, Fig. 2, left). Upon the addition of ~100 nM of a racemic mixture of the tetrahedral cage to the *cis*-side of the bilayer (Fig. 1A), temporal blockages of the ion current were observed at two discrete levels (I_b, grey bars in Fig. 2A). Data collated from multiple experiments that consisted of several thousand blockage events revealed two Gaussian distributions in the residual ion current (I_b/I_o), consistent with two distinct classes of blockage event. The possibility that these two classes arose from multiple cages interacting with the pore simultaneously was ruled out, since the ratio of the two events was independent of the overall cage concentration (Fig. S15, ESI†). Thus, the two classes of blockage in the presence of a racemic mixture of the ΛΛΛΛ and ΔΔΔΔ tetrahedral cages was consistent with our initial hypothesis that a protein nanopore may be able to discriminate supramolecular chirality at the single-molecule level.

Encouraged by these preliminary findings, we set out to confirm the ability of the approach to discriminate the chirality of tetrahedral cages. Enantiopure samples of both the ΛΛΛΛ and ΔΔΔΔ cages were obtained using established procedures.[37,40] Pleasingly, only one discrete blockage event class was observed for each enantiopure ΛΛΛΛ and ΔΔΔΔ cage sample (Fig. 2B and C). Moreover, the residual currents of these individual peaks were coincident with the two classes of event observed for the racemic mixture (Fig. 2B and C *cf.* A). Hence, we confirmed that α-HL is capable of discriminating the opposing supramolecular chirality of two otherwise chemically identical Ga(III) tetrahedral cages.

Having established that the discrimination of supramolecular chirality was possible based on the current blockage, we sought to examine the underlying kinetics and thermodynamics of the recognition process, which might be expected to significantly differ between enantiomers. Indeed, single-molecule methods allow the direct observation of association/dissociation kinetics.[41] A series of nanopore analyses were performed in which the concentration of each chiral form of the tetrahedral cage was varied between 25 and 100 nM. Each nanopore analysis was performed at least three times at each concentration. Event durations and inter-event durations (τ_{off} and τ_{on} respectively) were plotted as frequency-count histograms and fitted to single exponential decay functions (Fig. S20 and 21, ESI†). For both enantiomers, τ_{off} was found to be independent of cage concentration, whereas τ_{on} was linearly dependent on concentration (Fig. 3). These concentration dependencies confirmed the bimolecular nature of the interaction between each tetrahedral cage and the nanopore.[18,42] Thus, the rate constants of dissociation, $k_{off} = 1/\tau_{off}$, and association, $k_{on} = 1/\tau_{on}$[cage], could be determined for each enantiomer (Table 1). Intuitively, the intrinsic diastereotopic nature of the α-HL·cage complex might be expected to result in markedly different binding characteristics. However, only marginally different k_{on}, k_{off} and K_a values were observed (Table 1). Thus, unambiguous assignment of cage chirality was only possible using ion current blockages that result from electrostatic and steric factors, which are difficult to predict.[43]

Although the geometry and dynamics of the α-HL·cage complex are not known, the relatively small magnitudes (I_b/I_o) and durations (<200 ms) of the blockage events, combined with the marginal differences in the rates of association and dissociation (Table 1), indicate that the coordination cages interact transiently with the *cis*-opening of the nanopore without completely entering or translocating.[45–47] The scaled diagram shown in Fig. 4A shows that the longest diameter of the cage (2.3 nm) is slightly narrower than the *cis*-opening of the pore (2.6 nm), but wider than the *trans*-opening (2.1 nm). However, the space filling model does not take into account the solvation shell surrounding both the protein and the highly-charged cage. Indeed, dynamic light scattering experiments gave a hydrodynamic diameter of 2.5 ± 0.7 nm for the cage in D_2O (Fig. 4B). Thus, the size analysis and the characteristics of the blockage events indicate that entry of the cage into the wider vestibule of the pore is largely occluded. Nonetheless, deeper current blockages were occasionally observed that often lasted for tens of seconds under a continued applied potential. Such deeper events were distinct from non-specific gating events and showed a qualitative concentration dependence, suggesting that they may have arisen from inclusion of the cage within the vestibule of the pore (Fig. S10–13, ESI†). In contrast, no significant current blockages were observed when cages were added to the opposite side of the membrane that contained the even narrower *trans*-opening of the α-HL pore (Fig. 4 and S14, ESI†). Interestingly, the ability of ion current to discriminate the supramolecular chirality of a proportionally large cage species during transient interactions with the *cis*-entrance of the pore, rather than inclusion within the pore, raises the intriguing possibility that protein nanopores may provide a platform for the analysis of even larger constructs at the single-molecule level.

Significantly, the single-molecule nature of the approach enables facile *in situ* determination of enantiopurities. Since the k_{on} of each enantiomer can be determined from a racemic mixture of enantiomers that populate discrete current levels, then the concentration of each enantiomer can be determined by simply counting events. Eqn (1) describes the general

Table 1 Residual ion currents, kinetic and thermodynamic data for α-HL·cage complexation determined from nanopore experiments performed in 1 M KCl, 30 mM Tris–DCl, pD 7.6 in D_2O at 293 ± 2 K with an applied potential of +100 mV

	ΔΔΔΔ cage	ΛΛΛΛ cage
Residual current, I_b/I_o	0.76 ± 0.013	0.66 ± 0.011
Rate of association, $k_{on}/M^{-1}\ s^{-1}$	$7.5 \pm 0.3 \times 10^7$	$6.5 \pm 0.1 \times 10^7$
Rate of dissociation, k_{off}/s^{-1}	31 ± 3	35 ± 6
Association constant, K_a/M^{-1}	$2.4 \pm 0.3 \times 10^6$	$1.8 \pm 0.3 \times 10^6$

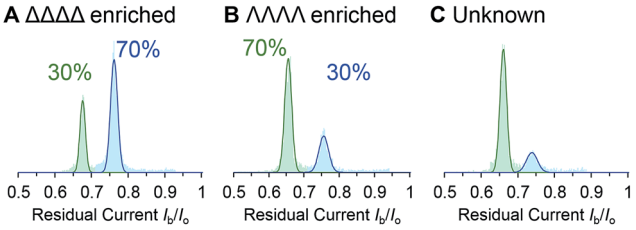

Fig. 5 (A–C) Event distributions generated for enantio-enriched samples. Experiments were performed in 1 M KCl, 30 mM Tris–DCl, pD 7.6 in D_2O at 293 ± 2 K with an applied potential of +100 mV.

Table 2 Determination of cage enantiomer concentrations in enantio-enriched samples

$\Delta : \Lambda_{actual}$[a]	30 : 70	30 : 70	70 : 30	70 : 30	Unknown
$[cage]_{total}$[a]/nM	77	102	77	102	50
Δ_{count}	1715	501	4763	3148	1723
Λ_{count}	3753	1060	2411	1565	425
$[\Delta]_{obs}$/nM	22 ± 2	30 ± 3	47 ± 5	65 ± 7	39 ± 4
$[\Lambda]_{obs}$/nM	55 ± 6	72 ± 7	28 ± 3	37 ± 4	11 ± 1
$\Delta : \Lambda_{obs}$	28 : 72	29 : 71	63 : 37	64 : 36	78 : 22

[a] Determined by ^{1}H NMR spectroscopy.

relationship between the event counts and the concentration of an individual enantiomer (see ESI† Section 4 for derivation).

$$[\Lambda] = \frac{\Lambda_{count} k_{on_\Delta}}{\Delta_{count} k_{on_\Lambda} + \Lambda_{count} k_{on_\Delta}} [cage]_{total} \quad (1)$$

We demonstrated the validity of this approach by determining the absolute concentrations of known mixtures of enantio-enriched samples (Fig. 5, Table 2 and ESI† Section 4). Furthermore, the technique proved useful during our own investigation by revealing that a sample that was intended to be enantiopure was, in fact, contaminated with 22% of the other enantiomer (Table 2, "Unknown" column). It is important to emphasise that the nanopore-based approach can determine the enantiopurity of a sample without a 100% pure reference sample, as required by ensemble analytical methods. Thus, we have established nanopore analysis as a complementary approach to existing methods such as circular dichroism[48,49] for the detection of supramolecular chirality.

Conclusions

In conclusion, we have demonstrated the general principle that an intrinsically chiral protein nanopore can serve as a detection element to discriminate the chirality of otherwise identical supramolecular entities. More specifically, we showed the magnitude of the ion current blockages arising from the transient association of tetrahedral Ga(III) cages with an α-haemolysin nanopore provided unambiguous assignment of the individual enantiomers. The single-molecule nature of the approach presents a distinct advantage over traditional ensemble-averaged techniques that cannot easily determine whether a sample is enantiopure or enantio-enriched, thus sidestepping the challenges associated with enantiopurification.[37,50–53] Direct access to kinetic parameters relating to the association/dissociation of individual cages with the nanopore allowed the concentrations of cage enantiomers to be determined from a single experiment on a timescale of minutes. Thus, such an approach may be amenable to the *in situ* analysis of dynamic supramolecular systems,[18,54] such as those associated with chiral amplification phenomena.[55–57] Significantly, the small magnitude of the observed current blockages was consistent with transient interactions with the pore opening rather than inclusion within the pore. As such, this preliminary study should encourage the future interrogation of even larger supramolecular architectures using nanopores.

Acknowledgements

We thank the Edinburgh Protein Purification Facility for equipment access and ERC Starting Grant 336935, "Transmembrane molecular machines" for funding.

Notes and references

‡ D_2O was used to enable NMR characterisation at all stages of the experiments.

1 E. M. Carreira and L. Kvaerno, *Classics in Stereoseletive Synthesis*, Wiley-VCH, 2008.
2 Y. Okamoto and T. Ikai, *Chem. Soc. Rev.*, 2008, **37**, 2593–2608.
3 K. Tanaka and N. Fukuda, *Tetrahedron: Asymmetry*, 2009, **20**, 111–114.
4 L. Yang, T. Wenzel, R. T. Williamson, M. Christensen, W. Schafer and C. J. Welch, *ACS Cent. Sci.*, 2016, **2**, 332–340.
5 M. Liu, L. Zhang and T. Wang, *Chem. Rev.*, 2015, **115**, 7304–7397.
6 M. A. Mateos-Timoneda, M. Crego-Calama and D. N. Reinhoudt, *Chem. Soc. Rev.*, 2004, **33**, 363–372.
7 A. Sorrenti, R. Rodriguez-Trujillo, D. B. Amabilino and J. Puigmartí-Luis, *J. Am. Chem. Soc.*, 2016, **138**, 6920–6923.
8 Q.-F. Sun, J. Iwasa, D. Ogawa, Y. Ishido, S. Sato, T. Ozeki, Y. Sei, K. Yamaguchi and M. Fujita, *Science*, 2010, **328**, 1144–1147.
9 R. Dickerson, H. Drew, B. Conner, R. Wing, A. Fratini and M. Kopka, *Science*, 1982, **216**, 475–485.
10 A. J. Wilson, *Chem. Soc. Rev.*, 2009, **38**, 3289–3300.
11 D. G. Blackmond, *Proc. Natl. Acad. Sci. U. S. A.*, 2004, **101**, 5732–5736.
12 P. L. Luisi, *The Emergence of Life: From Chemical Origins to Synthetic Biology*, Cambridge University Press, Cambridge, 2006.
13 J. Buratto, C. Colombo, M. Stupfel, S. J. Dawson, C. Dolain, B. Langlois d'Estaintot, L. Fischer, T. Granier, M. Laguerre, B. Gallois and I. Huc, *Angew. Chem., Int. Ed.*, 2014, **53**, 883–887.
14 M. Simon, M. Strathmann and N. Gautam, *Science*, 1991, **252**, 802–808.
15 A. Miyazawa, Y. Fujiyoshi and N. Unwin, *Nature*, 2003, **423**, 949–955.
16 M. De Poli, W. Zawodny, O. Quinonero, M. Lorch, S. J. Webb and J. Clayden, *Science*, 2016, **352**, 575–580.

17 F. G. A. Lister, B. A. F. Le Bailly, S. J. Webb and J. Clayden, *Nat. Chem.*, 2017, **9**, 420–425.
18 X.-f. Kang, S. Cheley, X. Guan and H. Bayley, *J. Am. Chem. Soc.*, 2006, **128**, 10684–10685.
19 A. J. Boersma and H. Bayley, *Angew. Chem., Int. Ed.*, 2012, **51**, 9606–9609.
20 M. B. Steffensen, D. Rotem and H. Bayley, *Nat. Chem.*, 2014, **6**, 603–607.
21 S.-H. Shin, M. B. Steffensen, T. D. W. Claridge and H. Bayley, *Angew. Chem., Int. Ed.*, 2007, **46**, 7412–7416.
22 L. Chen, W. Si, L. Zhang, G. Tang, Z.-T. Li and J.-L. Hou, *J. Am. Chem. Soc.*, 2013, **135**, 2152–2155.
23 B. B. Lakshmi and C. R. Martin, *Nature*, 1997, **388**, 758–760.
24 M. Ali, S. Nasir and W. Ensinger, *Electrochim. Acta*, 2016, **215**, 231–237.
25 Z. Sun, F. Zhang, X. Zhang, D. Tian, L. Jiang and H. Li, *Chem. Commun.*, 2015, **51**, 4823–4826.
26 C. Han, X. Hou, H. Zhang, W. Guo, H. Li and L. Jiang, *J. Am. Chem. Soc.*, 2011, **133**, 7644–7647.
27 C. Gao, S. Ding, Q. Tan and L.-Q. Gu, *Anal. Chem.*, 2009, **81**, 80–86.
28 D. L. Caulder, R. E. Powers, T. N. Parac and K. N. Raymond, *Angew. Chem., Int. Ed.*, 1998, **37**, 1840–1843.
29 L.-J. Chen, H.-B. Yang and M. Shionoya, *Chem. Soc. Rev.*, 2017, **46**, 2555–2576.
30 N. Ousaka, S. Grunder, A. M. Castilla, A. C. Whalley, J. F. Stoddart and J. R. Nitschke, *J. Am. Chem. Soc.*, 2012, **134**, 15528–15537.
31 A. M. Castilla, W. J. Ramsay and J. R. Nitschke, *Acc. Chem. Res.*, 2014, **47**, 2063–2073.
32 P. J. Stang, B. Olenyuk, D. C. Muddiman and R. D. Smith, *Organometallics*, 1997, **16**, 3094–3096.
33 S. P. Argent, T. Riis-Johannessen, J. C. Jeffery, L. P. Harding and M. D. Ward, *Chem. Commun.*, 2005, 4647–4649.
34 M. J. Burke, G. S. Nichol and P. J. Lusby, *J. Am. Chem. Soc.*, 2016, **138**, 9308–9315.
35 S. R. Seidel and P. J. Stang, *Acc. Chem. Res.*, 2002, **35**, 972–983.
36 T. R. Cook and P. J. Stang, *Chem. Rev.*, 2015, **115**, 7001–7045.
37 A. V. Davis, D. Fiedler, M. Ziegler, A. Terpin and K. N. Raymond, *J. Am. Chem. Soc.*, 2007, **129**, 15354–15363.
38 J. J. Kasianowicz, E. Brandin, D. Branton and D. W. Deamer, *Proc. Natl. Acad. Sci. U. S. A.*, 1996, **93**, 13770–13773.
39 M. A. Holden and H. Bayley, *J. Am. Chem. Soc.*, 2005, **127**, 6502–6503.
40 A. J. Terpin, M. Ziegler, D. W. Johnson and K. N. Raymond, *Angew. Chem., Int. Ed.*, 2001, **40**, 157–160.
41 L. Ma and S. L. Cockroft, *ChemBioChem*, 2010, **11**, 25–34.
42 O. Braha, J. Webb, L.-Q. Gu, K. Kim and H. Bayley, *ChemPhysChem*, 2005, **6**, 889–892.
43 S. F. Buchsbaum, N. Mitchell, H. Martin, M. Wiggin, A. Marziali, P. V. Coveney, Z. Siwy and S. Howorka, *Nano Lett.*, 2013, **13**, 3890–3896.
44 L. Song, M. R. Hobaugh, C. Shustak, S. Cheley, H. Bayley and J. E. Gouaux, *Science*, 1996, **274**, 1859–1865.
45 L.-Q. Gu, O. Braha, S. Conlan, S. Cheley and H. Bayley, *Nature*, 1999, **398**, 686–690.
46 J. Sánchez-Quesada, A. Saghatelian, S. Cheley, H. Bayley and M. R. Ghadiri, *Angew. Chem., Int. Ed.*, 2004, **43**, 3063–3067.
47 M. A. Watson and S. L. Cockroft, *Chem. Commun.*, 2015, **51**, 12243–12246.
48 L. A. Joyce, M. S. Maynor, J. M. Dragna, G. M. da Cruz, V. M. Lynch, J. W. Canary and E. V. Anslyn, *J. Am. Chem. Soc.*, 2011, **133**, 13746–13752.
49 D. Leung and E. V. Anslyn, *Org. Lett.*, 2011, **13**, 2298–2301.
50 K. Wu, K. Li, Y.-J. Hou, M. Pan, L.-Y. Zhang, L. Chen and C.-Y. Su, *Nat. Commun.*, 2016, **7**, 10487.
51 S. Wan, L.-R. Lin, L. Zeng, Y. Lin and H. Zhang, *Chem. Commun.*, 2014, **50**, 15301–15304.
52 C. Zhao, Q.-F. Sun, W. M. Hart-Cooper, A. G. DiPasquale, F. D. Toste, R. G. Bergman and K. N. Raymond, *J. Am. Chem. Soc.*, 2013, **135**, 18802–18805.
53 J. L. Bolliger, A. M. Belenguer and J. R. Nitschke, *Angew. Chem., Int. Ed.*, 2013, **52**, 7958–7962.
54 N. Ousaka, J. K. Clegg and J. R. Nitschke, *Angew. Chem., Int. Ed.*, 2012, **51**, 1464–1468.
55 F. Helmich, C. C. Lee, A. P. H. J. Schenning and E. W. Meijer, *J. Am. Chem. Soc.*, 2010, **132**, 16753–16755.
56 Y. Zhang, S. Li, M. Ma, M. Yang, Y. Wang, A. Hao and P. Xing, *New J. Chem.*, 2016, **40**, 5568–5576.
57 A. R. A. Palmans and E. W. Meijer, *Angew. Chem., Int. Ed.*, 2007, **46**, 8948–8968.